

Dynamical mass and multiplicity constraints on co-orbital bodies around stars

Dimitri Veras^{1*}, Thomas R. Marsh¹, Boris T. Gänsicke¹

¹*Department of Physics, University of Warwick, Coventry CV4 7AL, UK*

Accepted 2016 May 30. Received 2016 May 3; in original form 2016 February 22

ABSTRACT

Objects transiting near or within the disruption radius of both main sequence (e.g. KOI 1843) and white dwarf (WD 1145+017) stars are now known. Upon fragmentation or disintegration, these planets or asteroids may produce co-orbital configurations of nearly equal-mass objects. However, as evidenced by the co-orbital objects detected by transit photometry in the WD 1145+017 system, these bodies are largely unconstrained in size, mass, and total number (multiplicity). Motivated by potential future similar discoveries, we perform N -body simulations to demonstrate if and how debris masses and multiplicity may be bounded due to second-to-minute deviations and the resulting accumulated phase shifts in the osculating orbital period amongst multiple co-orbital equal point masses. We establish robust lower and upper mass bounds as a function of orbital period deviation, but find the constraints on multiplicity to be weak. We also quantify the fuzzy instability boundary, and show that mutual collisions occur in less than 5%, 10% and 20% of our simulations for masses of 10^{21} , 10^{22} and 10^{23} kg. Our results may provide useful initial rough constraints on other stellar systems with multiple co-orbital bodies.

Key words: minor planets, asteroids: general – stars: white dwarfs – methods: numerical – celestial mechanics – planet and satellites: dynamical evolution and stability – protoplanetary discs

1 INTRODUCTION

One recent exciting development in exoplanetary science has been the discovery of actively dying planets and asteroids. The main sequence stars KOI 2700, KIC 12557548B, and K2-22 all contain planet candidates which are thought to be disintegrating due to dusty flows or tails (Rappaport et al. 2012, 2014; Croll et al. 2014; Bochinski et al. 2015; Sanchis-Ojeda et al. 2015). These systems harbour objects with orbital periods of, respectively, about 22, 16 and 9 hours. The KOI 1843 system contains a planet candidate which, although not yet observed to be disintegrating, is close enough to its star’s disruption, or Roche, radius, for a lower bound on its density to be set at 7 g cm^{-3} (Rappaport et al. 2013). This object’s orbital period is only 4.245 hours.

These four systems provide just a taste of the widespread disruption which is assumed to occur around stars which have left the main sequence. In particular, between one quarter and one half of all known Milky Way white dwarfs possess atmospheres which are “polluted” from the metal-rich remnants of shorn-up plane-

tary systems (Zuckerman et al. 2003, 2010; Koester et al. 2014). The elemental profile of the pollution provides unique insight into planet formation and bulk chemical composition (Zuckerman et al. 2007; Klein et al. 2011; Gänsicke et al. 2012; Xu et al. 2014; Jura & Young 2014; Wilson et al. 2015, 2016), and accretion from dusty and sometimes gaseous debris discs likely gives rise to the pollution (Zuckerman & Becklin 1987; Gänsicke et al. 2006; Farihi et al. 2009; Bergfors et al. 2014; Wilson et al. 2014; Barber et al. 2016; Farihi 2016; Manser et al. 2016). The dynamical origin of these pollutants and their pathways through all stages of stellar evolution remains uncertain and represents a growing field of exploration (Veras 2016).

Although the tidal disruption of asteroids which veer into the Roche radius of the white dwarf has long been theorised to represent the dominant polluting mechanism (Graham et al. 1990; Jura 2003; Bonsor et al. 2011; Debes et al. 2012; Bear & Soker 2013; Frewen & Hansen 2014), visual confirmation of this process was not supplied until the discovery of transiting bodies orbiting WD 1145+017 (Vanderburg et al. 2015). Plentiful and ongoing follow-up observations of this system (Croll et al. 2015; Gänsicke et al. 2016; Rappaport et al. 2016; Alonso et al. 2016; Xu et al. 2016; Zhou et al. 2016) showcase complex

* E-mail: d.veras@warwick.ac.uk

dynamical signatures amongst at least six objects with orbital periods directly measured from photometric transit curves, sometimes with individual uncertainties as small as a few seconds. For main sequence stars, although co-orbital solid bodies have not yet been observed, an episode of catastrophic fragmentation might produce such bodies, leading to a similar architecture.

Such configurations raise fundamental questions about orbital dynamics, and about how mutual gravitational interactions may be linked to observations. Exquisite orbital period measurements belie the otherwise starkly unconstrained state of such systems: unknowns include the size, mass and multiplicity of the co-orbiting objects (henceforth referred to as just “bodies”), as well as the star’s mass. For a system like WD 1145+017, the size and mass of the bodies are unconstrained to within many orders of magnitude, whereas, because the star is a white dwarf, its mass is most likely to lie in the range $0.5M_{\odot} - 0.7M_{\odot}$ (e.g. Fig. 1 of Koester et al. 2014, and Tremblay et al. 2016). Regardless of these uncertainties, transit signatures strongly suggest that dust is emanating from the bodies, and Roche radius computations (e.g. based on equations and discussion from Murray & Dermott 1999; Cordes & Shannon 2008; Veras et al. 2014a; Bear & Soker 2015) affirm that the bodies are highly likely to be currently disintegrating.

Despite the unknowns, mutual interactions among the co-orbiting bodies can provide some theoretical constraints. These interactions will cause deviations in orbital period and ensuing accumulated phase shifts, both of which may be measurable. In this paper, we constrain the masses and multiplicities of co-orbital bodies in compact configurations by computing orbital period deviations with N -body numerical simulations. Although we use WD 1145+017 as inspiration, we do not attempt to specifically model this system because tidal disruption (Debes et al. 2012; Veras et al. 2014a), interaction with the extant disc (Rafikov 2011a; Metzger et al. 2012; Rafikov 2011b; Rafikov & Garmilla 2012) and rotational and orbital evolution due to white dwarf radiation (Veras et al. 2014b, 2015a,b,c; Stone et al. 2015) all likely play a role.

Instead, we perform simulations with an eye for future observations of similar systems around any type of star, in order to provide investigators with a basic notion of how orbital period deviations correspond to different architectures without complexities beyond point-mass gravitational dynamics. In Section 2, we briefly review co-orbital point mass dynamics with one central massive body. Section 3 presents our simulation setup and Section 4 displays our results. We conclude in Section 5.

2 CO-ORBITAL DYNAMICS

For nearly 250 years, researchers have attempted to understand how multiple objects may share the same orbit around a more massive primary (e.g. Lagrange 1772). A significant initial focus was the three-body problem, through which analytical stability formulae (Gascheau 1843; Routh 1875) proved reliable after the discovery of Trojan asteroids (Wolf 1906) and the only known pair of co-orbital satellites, Janus (Dollfus 1967) and Epimetheus (Fountain & Larson 1978). The more complex N -body co-orbital problem with $N > 3$

features a larger phase space, but has been studied primarily since the pioneering work of Maxwell (1890). He showed that in the limit of large N and for low-enough masses, stable rings may be achieved. For finite N , however, even if the bodies are symmetrically spaced, predicting the stability of the system becomes nontrivial (Pendse 1935; Salo & Yoder 1988).

Effectively, the case $N > 3$ requires numerical simulations unless the system in question can be linked to central configurations (Moeckel 1994; Renner & Sicardy 2004), a multi-body hierarchical restricted problem – which can be expressed entirely in terms of orbital element equations of motion – (Veras 2014a), or specialised symmetric cases (e.g. Bengochea et al. 2015). Few- or many-body co-orbital dynamics may also be informed by the periodic orbits of the $N = 3$ case (Hadjidemetriou et al. 2009; Hadjidemetriou & Voyatzis 2011; Antoniadou et al. 2014).

The discovery of extrasolar planets (Wolszczan & Frail 1992; Wolszczan 1994; Mayor & Queloz 1995) prompted a resurgence of interest in the co-orbital problem. Despite the absence of discoveries of Trojan planets around main sequence stars (but see Goździewski & Konacki 2006), the problem has received renewed attention in terms of planet formation and evolution (Nauenberg 2002; Kortenkamp et al. 2004; Schwarz et al. 2005; Beaugé et al. 2007; Cresswell & Nelson 2009; Izidoro et al. 2010; Smith & Lissauer 2010; Robutel & Pousse 2013; Pierens & Raymond 2014), Doppler radial velocity detections (Laughlin & Chambers 2002; Giuppone et al. 2012; Dobrovolskis 2013; Leleu et al. 2015), and detections by transit photometry (Ford & Gaudi 2006; Ford & Holman 2007; Janson 2013; Vokrouhlický & Nesvorný 2014; Placek et al. 2015) and binary eclipses (Schwarz et al. 2015).

This work differs from all of the above investigations due to the heretofore unforeseen character of the transit observations of polluted white dwarfs with disintegrating bodies (at least, as evidenced by WD 1145+017). Because we have no reason to believe that the bodies should be symmetrically spaced (see e.g. Fig. 3 of Gänsicke et al. 2016 and Fig. 6 of Rappaport et al. 2016) – despite this configuration being attractive analytically – we use N -body integrations to explore non-symmetrically-spaced bodies (along the same orbit). Our simulations primarily yield orbital period variations which can be compared to observations.

3 SIMULATION SETUP

For our explorations, we use a slightly-modified version of the N -body code MERCURY (Chambers 1999). The modifications include the effect of general relativity and better collision detection in the subroutine `mce_cent`, as was used in Veras et al. (2013) and Veras & Mustill (2013). These modifications are likely overkill; general relativity would advance the pericentre of circular co-orbital equal-mass bodies equally. Further, during each orbit, general relativity would cause the bodies to incur a maximum inward (non-cumulative) drift of just about 4-6 km (Veras 2014b).

We establish our initial conditions according to a scenario where K co-orbital bodies each of mass M orbit a star of mass M_* . Without loss of generality, we henceforth re-

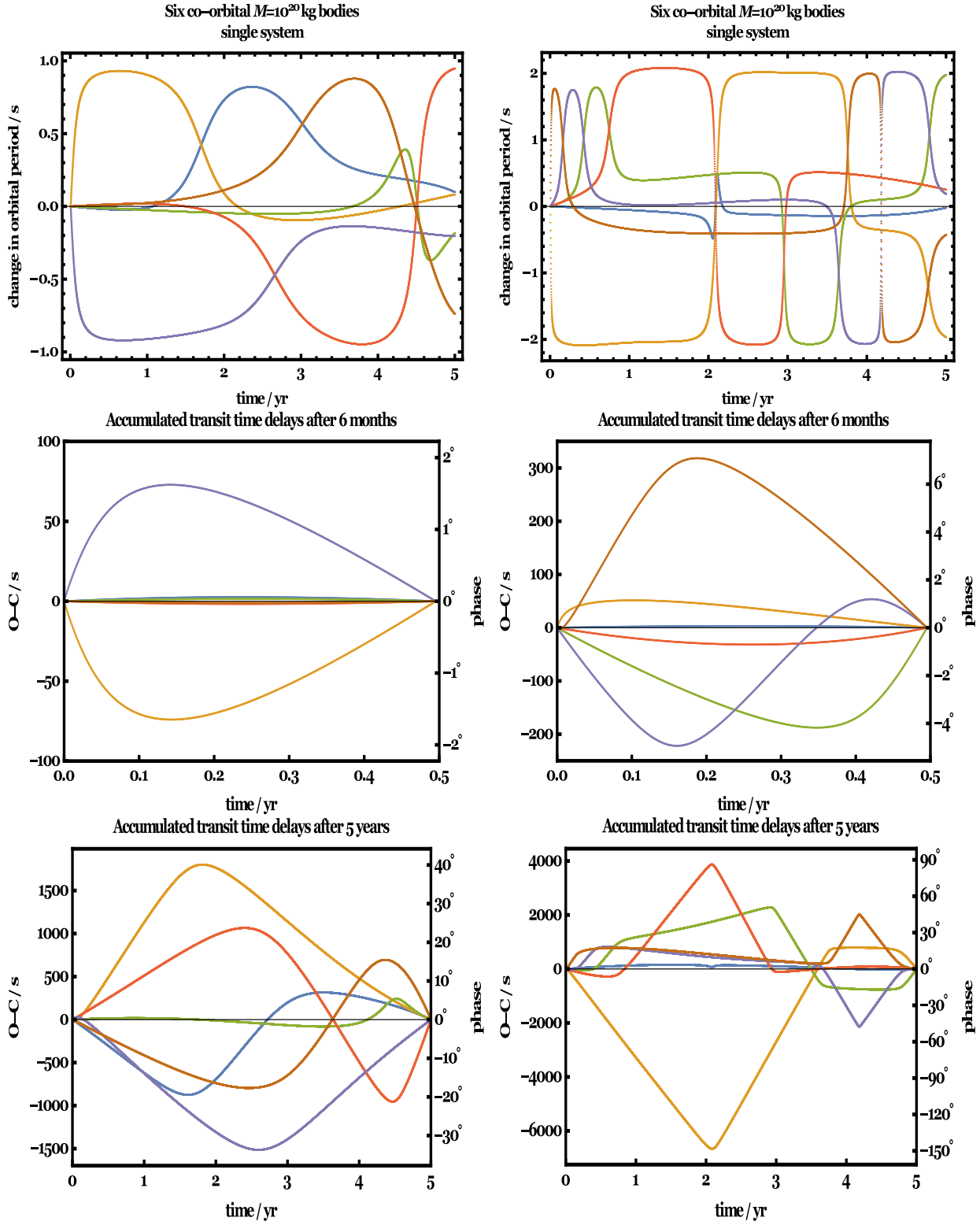


Figure 1. The variation in orbital period (*upper panels*) and O-C (observed - calculated) deviations of transit dip times from a linear ephemeris (*middle and lower panels*) for two systems of six 10^{20} kg co-orbital bodies whose orbits share an initial period of 4.49300 hours. The initial mean anomalies for all simulations in this paper were selected from a uniform random distribution; shown here are two cases with clustered sets of initial mean anomalies of about *left panels*: 176.3° , 219.4° , 238.5° , 253.1° , 262.3° and 292.7° , and *right panels*: 121.0° , 251.9° , 273.9° , 293.1° , 304.7° and 305.6° . Despite the similarity in these number sets, the left and right panels exhibit distinctive behaviour and amplitudes. Both systems would be detectable with current technology.

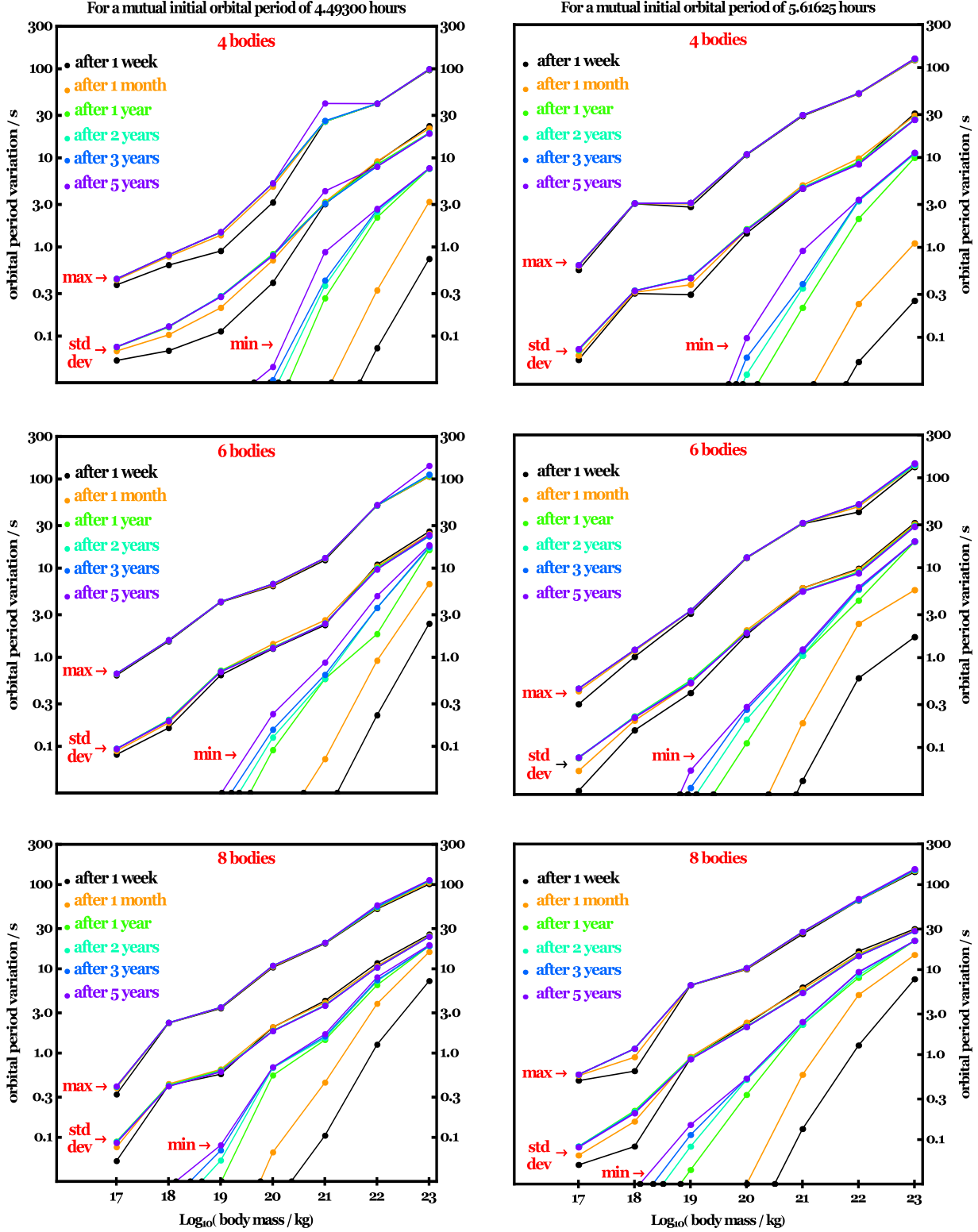


Figure 3. Bounding the mass of co-orbital bodies. The maximum and minimum orbital period deviations (upper and lower curves, respectively, in each plot) for our suites of simulations effectively provide the lower and upper mass bounds, for a given number of bodies (4, top; 6, middle; 8, bottom), initial orbital periods (left, 4.49300 hours; right, 5.61625 hours), and sampling times (labelled different colours). We also provide the standard deviation of orbital period deviation in the middle set of curves. To first order, the plots are insensitive to multiplicity, and are strongly dependent on co-orbital body mass.

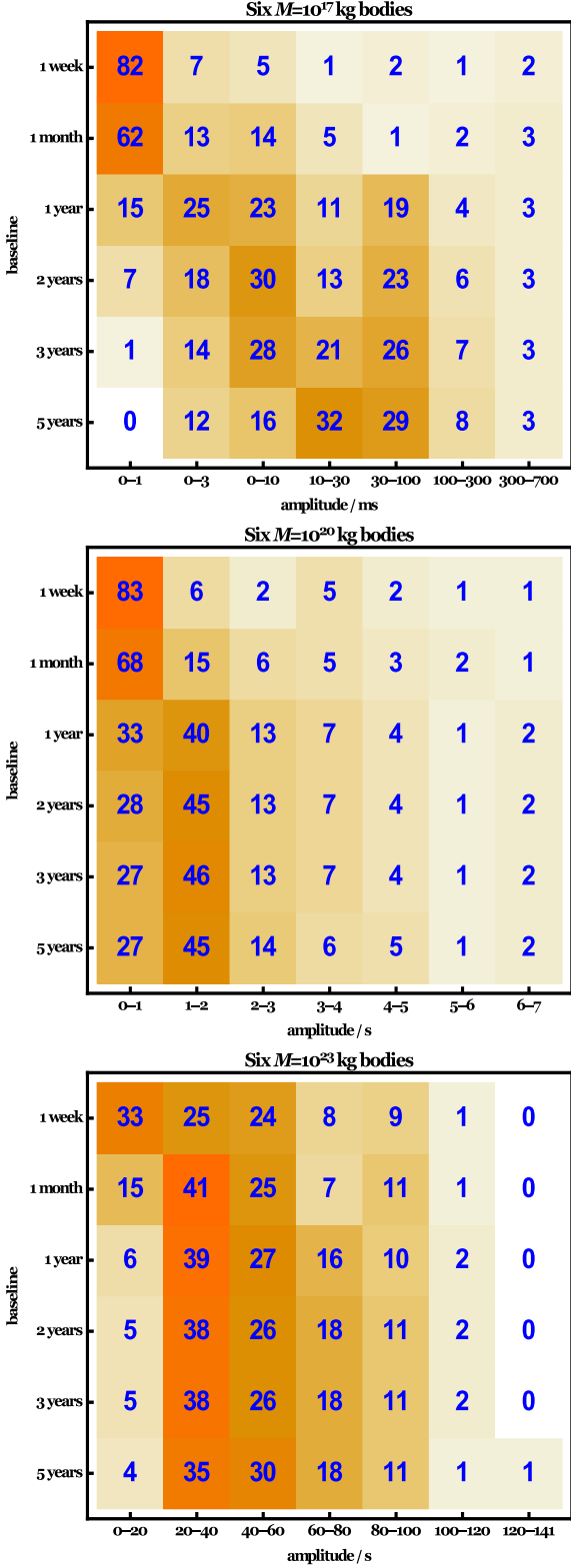


Figure 2. The number of systems (embedded blue numbers) for which a particular maximum orbital period variation occurred (x -axes) over a given baseline of observations (y -axes) for suites of 100 stable simulations of six co-orbital bodies with masses 10^{17} kg (upper panel), 10^{20} kg (middle panel), and 10^{23} kg (lower panel). The initial orbital periods of all bodies are 4.49300 hours. Both systems from Fig. 1, sampled after 5 years, fall in the corresponding 1-2 second amplitude tile in the middle panel here.

fer to the star as a white dwarf. The initial mutual orbit of the bodies is circular with semimajor axis a . For each set of (K, M, M_*, a) , we run over 100 simulations such that each one features bodies whose initial mean anomalies are drawn from a uniform random distribution. We run just enough simulations per set such that exactly 100 remain stable for the duration of five years (we also keep and count the unstable simulations for later analysis). We output data every 0.25 day, and report orbital period variations after one week (defined as seven days), one month (defined as 30 days), one year (defined as 365 days), two years, three years and five years.

We sample all permutations of (K, M, M_*, a) where $K = \{4, 6, 8\}$ and $M = \{10^{17}, 10^{18}, 10^{19}, 10^{20}, 10^{21}, 10^{22}, 10^{23}\}$ kg. For the sake of adopting a stellar mass and period of the co-orbital body, we adopt the values for WD 1145+017, i.e. $M_* = 0.60M_\odot$, and $P = 4.49300$ hours, as well as a value 25% larger ($P = 5.61625$ hours). We note that the white dwarf mass in WD1145+017 is not yet accurately known, and that these parameters are equally illustrative for close-in planets at main sequence stars (e.g. for KOI 1843.03, with $M_* = 0.46M_\odot$ and $P = 4.245$ hours; Rappaport et al. 2013). For a given P , the values of a change strictly according to what M is being sampled.

The value of 10^{23} kg represents a realistic upper bound for individual masses of co-orbital bodies which we might expect. Planet-mass objects are rarely thought to enter the white dwarf Roche radius (Veras et al. 2013; Mustill et al. 2014), particularly for large planets (Veras & Gänsicke 2015; Veras et al. 2016a). The probability, however, increases for asteroid-sized (Bonsor et al. 2011; Bonsor & Wyatt 2012; Debes et al. 2012; Frewen & Hansen 2014; Bonsor & Veras 2015) or moon-sized (Payne et al. 2016a,b) bodies, given the presence of eccentric planets (Antoniadou & Veras 2016); comets enter the Roche radius approximately once every 10^4 years (Alcock et al. 1986; Veras et al. 2014d) but are subject to quick evaporation (Stone et al. 2015; Veras et al. 2015b; Brown, Veras & Gänsicke 2016). Further, planets are complex multi-layered objects whose tidal disruption around main sequence stars (Guillochon et al. 2011; Liu et al. 2013) implies that dedicated treatments would be necessary for white-dwarf-based studies.

Although all bodies in our simulations are treated with point mass dynamics, we give the white dwarf a finite fiducial radius of 8750 km in order to detect any potential collisions with bodies. As M increases, we would expect instability to occur on a more frequent basis, and this instability can manifest as collisions between bodies, collisions between a body and the white dwarf, and ejections. We set the ejection radius at 3×10^5 au, which represents a reasonable upper bound on each axis of the true Hill ellipsoid of planetary systems in the Solar neighbourhood (Veras & Evans 2013; Veras et al. 2014c). The duration of our simulations (5 yr) ensures that no scattered object would actually have time to reach this edge, but this value allows any object on its way out to be retained and tracked.

4 RESULTS

Our simulations yield osculating values of each body’s orbital elements, as well as indications about which have remained stable. Of greatest interest is the osculating semi-major axis, which can be converted to orbital period, a direct observable in transiting systems. Subsections 4.1 and 4.2 showcase the results for orbital period variations and instability, respectively. Subsection 4.3 then assesses the applicability of these results to the WD 1145+017 system.

4.1 Orbital period variations

Each body varies its orbital period in a non-trivial manner due to the number and distribution of objects in each system. Consequently, we rely on statistics to make gross characterisations. For an individual observed system, if the phases of each object are known, then a more focused study may be carried out. Such investigations may also consider bodies hidden from view which may significantly contribute to orbital period variations.

We illustrate two examples of the nonuniformity of the orbital period variations in Fig. 1. Both systems in the figure adopt ($K = 6$, $M = 10^{20}$ kg, $M_\star = 0.6M_\odot$, $a = 0.00535$ au) – where we have used the WD 1145+017 system as a guide (Gänsicke et al. 2016; Rappaport et al. 2016) – but with different initial mean anomalies (both randomly chosen sets of initial phases). The top panels show how the amplitude and other properties of these periods vary with time, so that the period variation is a function of observing baseline. The top panels also illustrate different behaviour from each other: the evolution in the right panel exhibits quicker amplitude changes from the left panel.

The bottom two panels on each side of the figure are “O-C” (Observed - Calculated) diagrams. They illustrate how, for these two sets of parameters in particular, the times of the observed transit dips deviate from a linear dependence on orbital phase (ephemeris). Observations are more sensitive to relative phase shifts than the actual period variation, provided that individual transits are unambiguously identified over a sufficiently long baseline of observations. The middle and bottom panels, respectively, illustrate the deviations from linearity in transit time after six months and five years. The five-year cases represent the full baseline of simulations, whereas the six-month cases represent perhaps more realistic scenarios. In all four cases, the deviations are large enough to be detected. The extent of the deviation can vary by a factor of three even though the initial phases are similarly clustered (see figure caption).

The matrix plots in Fig. 2 show how commonly systems with a given mass of co-orbiting bodies and time baseline achieve particular maximum period deviations. The colours indicate the magnitude of the number of systems out of 100 that achieve amplitudes in a range whose maximum extent was found to be 0.7 seconds (upper panel, for $M = 10^{17}$ kg), 7 seconds (middle panel, for $M = 10^{20}$ kg) and 141 seconds (lower panel, for $M = 10^{23}$ kg). There does not exist one necessarily representative distribution (or colour scheme) for all sets of (K , M , M_\star , a). Outliers are the result of special configurations of multi-body co-orbital problems, such as 60° offsets for the much simpler $K = 2$ case under the guise of the restricted three-body problem.

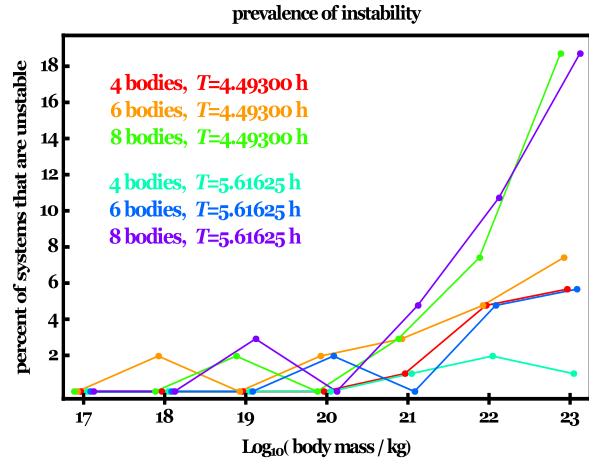


Figure 4. Fraction of unstable systems for different combinations of multiplicity, mass and orbital period. Each data point is slightly horizontally offset for clarity. In at least 95%, 90% and 80% of all simulations, masses under 10^{21} , 10^{22} and 10^{23} kg respectively kept the systems stable. Consequently, in general terms, instability does not provide as robust a bound on the masses as does the maximum and minimum period deviations (Fig. 3).

In aggregate, however, over the entire phase space there exist clear trends, which are displayed in Fig. 3. That figure is particularly important because it effectively bounds the masses from above and below with the bottom and top sets of curves. These sets correspond to the minimum and maximum period deviations obtained in any of the stable simulations that were run; the middle curves display the standard deviation.

From these curves, also note (i) the clear upward trend in orbital period variation as a function of M , (ii) the slight increase in maximum deviation values for the larger P value (right panels), and (iii) the upper and middle sets of curves in each plot are largely insensitive to the sampling timescale, unlike the lower curves. This trend may be inferred from Fig. 1.

4.2 Instability

One potential constraint on the upper mass bound of bodies is system stability. Although instability may come in the form of engulfments within the star, bodies being perturbed on a course out of the system, or collisions amongst bodies, only the last possibility occurred in our simulations. The likely reason is because any close encounters between the bodies, given their masses, could not have generated the speed needed to eventually escape the system. Further, co-orbital circular configurations are geometrically unfavoured to produce ejections or engulfments within the parent star. Therefore, even if we had instead adopted a stellar radius that was commensurate with a small main sequence star, engulfments would still not have been likely to occur unless the co-orbital bodies were large enough to be affected by star-planet tides.

There does not exist a particular critical body mass at which a system would go unstable because stability is a function of both K and M for a fixed number of orbits. Nev-

ertheless, the probability of instability increases as both K and M do, as demonstrated by Fig. 4. The plot makes clear predictions that instability should occur under the 5%, 10% and 20% level for $M \leq 10^{21}, 10^{22}$ and 10^{23} kg. Regarding bounding body masses from observations, these constraints are weak compared to those obtained from orbital period deviations.

Finally, we note that collisions amongst bodies might be observable. The result will be a reduced value of K , and a change in orbital period variations. In this scenario, however, the masses of the remaining co-orbital bodies are no longer likely to be equal, and consequently a more detailed analysis would be required.

4.3 Comparison to WD 1145+017

As suggested in the introduction, the WD 1145+017 system is too complex to be modelled by the architecture and masses that we have adopted here. Nevertheless, one interesting comparison can be made: typical orbital period deviations that are reported in this study for $M = 10^{20}$ kg are roughly a few seconds (Fig. 3). Rappaport et al. (2016) deduced that an asteroid mass of this order of magnitude can, through fragmentation, produce bodies which settle into an orbit whose period deviates from the original orbit by about 27 seconds. This larger, observed, deviation in WD 1145+017 may easily be explained by effects not accounted for here, which include (i) the orbiting objects are probably of different mass, (ii) the process of fragmentation, (iii) the known presence of dust, and (iv) the known presence of gas.

5 SUMMARY

Multiple co-orbital bodies near or inside of a stellar Roche radius might provide unique insights into a system's violent history. For white dwarfs, these bodies provide a glimpse into how debris discs are formed and how white dwarf atmospheres are polluted. The mutual perturbations amongst the bodies generate slight variations in orbital periods ($\sim 0.1 - 100$ s) and phase shifts over the course of weeks, months or years, which are detectable by current instruments. Here, we have quantified this variation as a function of mass, multiplicity, distance and time sampling (Fig. 3) and show that for a given orbital period deviation, lower and upper mass bounds may be estimated. We also characterised the fuzzy instability boundary (Fig. 4), which provides an upper bound on the incidence of instability for a given co-orbital body mass.

ACKNOWLEDGEMENTS

We thank the referee for their useful feedback on this manuscript. DV and BTG have received funding from the European Research Council under the European Union's Seventh Framework Programme (FP/2007-2013)/ERC Grant Agreement n. 320964 (WDTracer). TRM was supported under a Science and Technology Facilities Council (STFC) grant, ST/L000733.

REFERENCES

- Alcock, C., Frstrom, C. C., & Siegelman, R. 1986, *ApJ*, 302, 462
- Alonso, R., Rappaport, S., Deeg, H. J., & Palles, E. 2016, In Press, *A&A*, arXiv:1603.08823
- Antoniadou, K. I., Voyatzis, G., & Varvoglis, H. 2014, *IAU Symposium*, 310, 82
- Antoniadou, K. I., Veras, D. 2016, Submitted to *MNRAS*
- Barber, S. D., Belardi, C., Kilic, M., & Gianninas, A. 2016, *MNRAS*, 459, 1415
- Bear, E., & Soker, N. 2013, *New Astronomy*, 19, 56
- Bear, E., & Soker, N. 2015, *MNRAS*, 450, 4233
- Beaugé, C., Sándor, Z., Érdi, B., Süli, Á. 2007, *A&A*, 463, 359
- Bengochea, A., Galán, J., & Pérez-Chavela, E. 2015, *Physica D Nonlinear Phenomena*, 301, 21
- Bergfors, C., Farihi, J., Dufour, P., & Rocchetto, M. 2014, *MNRAS*, 444, 2147
- Bochinski, J. J., Haswell, C. A., Marsh, T. R., Dhillon, V. S., & Littlefair, S. P. 2015, *ApJL*, 800, L21
- Bonsor, A., Mustill, A. J., & Wyatt, M. C. 2011, *MNRAS*, 414, 930
- Bonsor, A., & Wyatt, M. C. 2012, *MNRAS*, 420, 2990
- Bonsor, A., & Veras, D. 2015, *MNRAS*, 454, 53
- Brown, J. C., Veras, D., Gänsicke, B. T. 2016, In prep
- Chambers, J. E. 1999, *MNRAS*, 304, 793
- Cordes, J. M., & Shannon, R. M. 2008, *ApJ*, 682, 1152
- Cresswell, P., & Nelson, R. P. 2009, *A&A*, 493, 1141
- Croll, B., Rappaport, S., DeVore, J., et al. 2014, *ApJ*, 786, 100
- Croll, B., Dalba, P. A., Vanderburg, A., et al. 2015, arXiv:1510.06434
- Debes, J. H., Walsh, K. J., & Stark, C. 2012, *ApJ*, 747, 148
- Dobrovolskis, A. R. 2013, *Icarus*, 226, 1635
- Dollfus, A. 1967, *Sky & Telescope*, 34,
- Farihi, J., Jura, M., & Zuckerman, B. 2009, *ApJ*, 694, 805
- Farihi, J. Submitted to *New Astronomy Reviews*
- Ford, E. B., & Gaudi, B. S. 2006, *ApJL*, 652, L137
- Ford, E. B., & Holman, M. J. 2007, *ApJL*, 664, L51
- Fountain, J. W., & Larson, S. M. 1978, *Icarus*, 36, 92
- Frewen, S. F. N., & Hansen, B. M. S. 2014, *MNRAS*, 439, 2442
- Gänsicke, B. T., Marsh, T. R., Southworth, J., & Rebassa-Mansergas, A. 2006, *Science*, 314, 1908
- Gänsicke, B. T., Koester, D., Farihi, J., et al. 2012, *MNRAS*, 424, 333
- Gänsicke, B. T., Aungwerojwit, A., Marsh, T. R., et al. 2016, *ApJL*, 818, L7
- Gascheau, G. 1843, *C.R. Acad. Sci. Paris*, 16, 393
- Giuppone, C. A., Benítez-Llambay, P., & Beaugé, C. 2012, *MNRAS*, 421, 356
- Goździewski, K., & Konacki, M. 2006, *ApJ*, 647, 573
- Graham, J. R., Matthews, K., Neugebauer, G., & Soifer, B. T. 1990, *ApJ*, 357, 216
- Guillochon, J., Ramirez-Ruiz, E., & Lin, D. 2011, *ApJ*, 732, 74
- Hadjidemetriou, J. D., Psychoyos, D., & Voyatzis, G. 2009, *Celestial Mechanics and Dynamical Astronomy*, 104, 23
- Hadjidemetriou, J. D., & Voyatzis, G. 2011, *Celestial Mechanics and Dynamical Astronomy*, 111, 179
- Izidoro, A., Winter, O. C., & Tsuchida, M. 2010, *MNRAS*,

- 405, 2132
- Janson, M. 2013, *ApJ*, 774, 156
- Jura, M. 2003, *ApJL*, 584, L91
- Jura, M., & Young, E. D. 2014, *Annual Review of Earth and Planetary Sciences*, 42, 45
- Klein, B., Jura, M., Koester, D., & Zuckerman, B. 2011, *ApJ*, 741, 64
- Koester, D., Gänsicke, B. T., & Farihi, J. 2014, *A&A*, 566, A34
- Kortenkamp, S. J., Malhotra, R., & Michtchenko, T. 2004, *Icarus*, 167, 347
- Lagrange, J-L. 1772 *Œuvres complètes* (Paris: Gouthier-Villars)
- Laughlin, G., & Chambers, J. E. 2002, *AJ*, 124, 592
- Leleu, A., Robutel, P., & Correia, A. C. M. 2015, *A&A*, 581, A128
- Liu, S.-F., Guillochon, J., Lin, D. N. C., & Ramirez-Ruiz, E. 2013, *ApJ*, 762, 37
- Manser, C. J. Gänsicke, B. T., Marsh, T. R., et al. 2016, *MNRAS*, 455, 4467
- Maxwell, C. J. 1890 On the stability of the motion of Saturn's Rings, in *Scientific Papers of James Clerk Maxwell*, Cambridge University Press, Vol 1, 228.
- Mayor, M., & Queloz, D. 1995, *Nature*, 378, 355
- Metzger, B. D., Rafikov, R. R., & Bochkarev, K. V. 2012, *MNRAS*, 423, 505
- Moeckel, R. 1994, *J. Dyn. Diff. Eq.*, 6(1), 35
- Murray, C. D., & Dermott, S. F. 1999, *Solar system dynamics*
- Mustill, A. J., Veras, D., & Villaver, E. 2014, *MNRAS*, 437, 1404
- Nauenberg, M. 2002, *AJ*, 124, 2332
- Payne, M. J., Veras, D., Holman, M. J., Gänsicke, B. T. 2016a, *MNRAS*, 457, 217
- Payne, M. J., Veras, D., Gänsicke, B. T., Holman, M. J., 2016b, Submitted to *MNRAS*
- Pendse, C. G. 1935, *Phil. Trans. Roy. Soc. London (A)*, 234, 145
- Pierens, A., & Raymond, S. N. 2014, *MNRAS*, 442, 2296
- Placek, B., Knuth, K. H., Angerhausen, D., & Jenkins, J. M. 2015, *ApJ*, 814, 147
- Rafikov, R. R. 2011a, *MNRAS*, 416, L55
- Rafikov, R. R. 2011b, *ApJL*, 732, LL3
- Rafikov, R. R., & Garmilla, J. A. 2012, *ApJ*, 760, 123
- Rappaport, S., Levine, A., Chiang, E., et al. 2012, *ApJ*, 752, 1
- Rappaport, S., Sanchis-Ojeda, R., Rogers, L. A., Levine, A., & Winn, J. N. 2013, *ApJ*, 773, L15
- Rappaport, S., Barclay, T., DeVore, J., et al. 2014, *ApJ*, 784, 40
- Rappaport, S., Gary, B. L., Kaye, T., et al. 2016, *arXiv:1602.00740*
- Renner, S., & Sicardy, B. 2004, *Celestial Mechanics and Dynamical Astronomy*, 88, 397
- Robutel, P., & Pousse, A. 2013, *Celestial Mechanics and Dynamical Astronomy*, 117, 17
- Routh, E.J. 1875, *Proc. Lond. Math. Soc.*, 6, 86
- Salo, H., & Yoder, C. F. 1988, *A&A*, 205, 309
- Sanchis-Ojeda, R., Rappaport, S., Pallè, E., et al. 2015, *ApJ*, 812, 112
- Schwarz, R., Pilat-Lohinger, E., Dvorak, R., Érdi, B., & Sándor, Z. 2005, *Astrobiology*, 5, 579
- Schwarz, R., Bazsó, Á., Funk, B., & Zechner, R. 2015, *MNRAS*, 453, 2308
- Smith, A. W., & Lissauer, J. J. 2010, *Celestial Mechanics and Dynamical Astronomy*, 107, 487
- Stone, N., Metzger, B. D., & Loeb, A. 2015, *MNRAS*, 448, 188
- Tremblay, P.-E., et al., Submitted to *MNRAS*
- Vanderburg, A., Johnson, J. A., Rappaport, S., et al. 2015, *Nature*, 526, 546
- Veras, D., Mustill, A. J., Bonsor, A., & Wyatt, M. C. 2013, *MNRAS*, 431, 1686
- Veras, D., & Evans, N. W. 2013, *MNRAS*, 430, 403
- Veras, D., & Mustill, A. J. 2013, *MNRAS*, 434, L11
- Veras, D. 2014a, *Celestial Mechanics and Dynamical Astronomy*, 118, 315
- Veras, D. 2014b, *MNRAS*, 442, L71
- Veras, D., Leinhardt, Z. M., Bonsor, A., Gänsicke, B. T. 2014a, *MNRAS*, 445, 2244
- Veras, D., Jacobson, S. A., Gänsicke, B. T. 2014b, *MNRAS*, 445, 2794
- Veras, D., Evans, N. W., Wyatt, M. C., & Tout, C. A. 2014c, *MNRAS*, 437, 1127
- Veras, D., Shannon, A., Gänsicke, B. T. 2014d, *MNRAS*, 445, 4175
- Veras, D., Gänsicke, B. T. 2015, *MNRAS*, 447, 1049
- Veras, D., Eggl, S., Gänsicke, B. T. 2015a, *MNRAS*, 451, 2814
- Veras, D., Eggl, S., Gänsicke, B. T. 2015b, *MNRAS*, 452, 1945
- Veras, D., Leinhardt, Z. M., Eggl, S., Gänsicke, B. T. 2015c, *MNRAS*, 451, 3453
- Veras, D. 2016, *Royal Society Open Science*. 3:150571
- Veras, D., Mustill, A. M., Gänsicke, B. T., Redfield, S., Georgakarakos, N., Bowler, A. B., Lloyd, M. J. S. 2016a, Submitted to *MNRAS*
- Vokrouhlický, D., & Nesvorný, D. 2014, *ApJ*, 791, 6
- Wilson, D. J., Gänsicke, B. T., Koester, D., et al. 2014, *MNRAS*, 445, 1878
- Wilson, D. J., Gänsicke, B. T., Koester, D., et al. 2015, *MNRAS*, 451, 3237
- Wilson, D. J., Gänsicke, B. T., Farihi, J., & Koester, D. 2016, *MNRAS*, 459, 3282
- Wolf, M. 1906, *Astron. Nachr.*, 170, 353
- Wolszczan, A., & Frail, D. A. 1992, *Nature*, 355, 145
- Wolszczan, A. 1994, *Science*, 264, 538 wolszczan
- Xu, S., Jura, M., Koester, D., Klein, B., & Zuckerman, B. 2014, *ApJ*, 783, 79
- Xu, S., Jura, M., Dufour, P., & Zuckerman, B. 2016, *ApJL*, 816, L22
- Zhou, G., Kedziora-Chudczer, L., Bailey, J., et al. 2016, Submitted to *MNRAS*, *arXiv:1604.07405*
- Zuckerman, B., & Becklin, E. E. 1987, *Nature*, 330, 138
- Zuckerman, B., Koester, D., Reid, I. N., Hüensch, M. 2003, *ApJ*, 596, 477
- Zuckerman, B., Koester, D., Melis, C., Hansen, B. M., & Jura, M. 2007, *ApJ*, 671, 872
- Zuckerman, B., Melis, C., Klein, B., Koester, D., & Jura, M. 2010, *ApJ*, 722, 725